NMR study of the quasi-reorientational dynamics of Li ions in $KTaO_3$:Li

J. J. van der Klink
Institut de Physique Expérimentale, Ecole Polytechnique Fédérale de Lausanne (Swiss Federal Institute of Technology), CH-1015 Lausanne, Switzerland

F. Borsa
Istituto di Fisica dell'Università degli Studi di Pavia e Unità Gruppo Nazionale di Struttura della Materia del Consiglio Nazionale delle Ricerche, I-27100 Pavia, Italy

(Received 1 March 1984)

Measurements of static quadrupole effects on the NMR spectrum and of nuclear spin-lattice relaxation both in the laboratory frame, T_1^{-1}, and in the rotating frame, $T_{1\rho}^{-1}$, are reported for ^{7}Li, ^{39}K, and ^{181}Ta nuclei in $KTaO_3$:Li mixed crystals as a function of Li concentration and of temperature. The aim of the present investigation is to clarify the role of the Li dynamics in the low-temperature phase transition, which has been ascribed either to a dipole-glass-type condensation or to a ferroelectric transition. Both the quadrupole splitting of the ^{7}Li NMR spectrum and the T_1^{-1} of ^{7}Li and ^{39}K versus T indicate that for all concentrations investigated, the Li-dipole dynamics is dominated by thermally activated hopping among off-center positions displaced by 1.26 Å along the [100] directions. The ^{7}Li $T_{1\rho}^{-1}$-versus-T data and the disappearance of the ^{181}Ta NMR signal indicate, instead, that a small degree of preferential orientation develops even at high temperature and that it decays on a much longer time scale than the thermally activated hopping. No anomaly in either T_1^{-1} or in the NMR spectrum is observed for ^{7}Li and ^{39}K at the transition temperature. However, a tetragonal distortion with $(c-a)/a < 0.007$ is still consistent with the data. Finally a detailed account is given for the nonexponential recovery of the ^{7}Li nuclear magnetization in presence of spin-lattice and spin-spin interactions of the same order of magnitude and for the expression of the correlation function in presence of the postulated two—time-scale Li dynamics.

I. INTRODUCTION

When a Li ion substitutes for K in $KTaO_3$ it takes up an off-center position with respect to the cubic site, along one of the six ⟨100⟩ directions. The local electric dipole thus created can accordingly have six possible orientations, and at sufficiently high temperatures thermally activated hopping occurs between orientations related through 90° jumps. Birefringence and dielectric susceptibility experiments have shown[1] that collective effects between the dipoles exist at low temperatures and sufficiently high Li concentration, leading to the definition of a glass-type transition temperature. At the same time, other experiments such as Raman and Brillouin scattering,[2] and again birefringence,[3,4] tend to favor an interpretation in terms of a normal ferroelectric transition. In ordinary ferroelectric-type transitions it is experimentally well established that the slowing down induces a critical behavior of the spin-lattice relaxation rate as the transition temperature is approached.[5] Also, below T_c, the size of the static quadrupole effects is simply related to the magnitude of the order parameter.[5] Neither of the above-mentioned effects is observed in the ^{7}Li NMR study of $KTaO_3$:Li crystals.[1]

The rather detailed theoretical analysis of the nuclear magnetic resonance and relaxation of ^{7}Li, ^{39}K, and ^{181}Ta in $KTaO_3$:Li that we present in this paper is an attempt to give a quantitative description of the local Li dynamics as this appear to be of paramount importance in understanding the nature of the phase transition.

A most characteristic feature of the experimental spin-lattice relaxation curves for ^{7}Li is their nonexponentiality; also characteristic is their dependence upon the orientation of the Zeeman field with respect to the crystal axes. The nonexponential decay implies that the spin-spin interactions are too weak to maintain a unique spin temperature: the relaxation is governed by quadrupolar interactions of single nuclei. We will therefore develop an expression for quadrupolar relaxation in the presence of spin-spin interactions that are not necessarily weak or strong compared to the spin-lattice coupling: One limit of the expression obtained gives the familiar single-exponential spin-temperature result, whereas another limit yields the double-exponential decay also found, e.g., in viscous liquids. From comparison with experiment we will see that both limits can be encountered in $KTaO_3$:Li, depending upon temperature. When the motion slows down towards lower temperature, quadrupolar splittings start to appear in the spectrum. These are determined by the same parameters as the relaxation, and the shape of the spectrum can be calculated from a "three-site exchange" model. A quantitative comparison of theoretical and experimental results is difficult here, but we will show that the qualitative agreement is satisfactory. These aspects of the problem, which are mainly of NMR technical character, are developed in Sec. III.

The temperature behavior of most of the NMR parameters is largely dominated by the Li thermal hopping

among the six equivalent positions. This type of dynamics is determined by single-particle properties, and the low-temperature "freezing" of the individual dipoles is simply associated with the slowing down of the thermal hopping. On the other hand, we find that the temperature behavior of some specific NMR parameters, namely the ^{7}Li spin-lattice relaxation rate in the rotating frame $T_{1\rho}^{-1}$ and the ^{181}Ta signal intensity, can be understood only by invoking a more complex dynamics. Thus, in Sec. IV we develop a theoretical model for the Li dynamics based on a two—time-scale decay for the position-position correlation function which enters the expressions for the relaxation rates. The model implies that, locally, the Li hops fast among the the six equivalent positions (three equivalent axes), but that the residence time on each site is not identical, giving rise to a preferential ordering along one axis which decays slowly in time. The anisotropy of the local motion can be related in a natural way to the formation of slowly decaying polarization clusters associated with the interactions among the random dipoles. In Sec. V we present an interpretation of the experimental results based mostly on the two—time-scale dynamics followed in Sec. VI by some concluding remarks.

II. EXPERIMENTAL RESULTS

We have observed nuclear-magnetic-resonance signals of ^{7}Li, ^{39}K, and ^{181}Ta in several crystals of $K_{1-x}Li_xTaO_3$. Some properties of the ^{7}Li resonance have already been mentioned in previous papers,[4,6] but it seems useful to give a brief recapitulation, since most of the theory we will develop applies specifically to this resonance. The ^{39}K and ^{181}Ta signals have been studied in less detail, but it is important to show that their behavior is consistent with the model proposed in Sec. IV. For all nuclei, pulsed-NMR methods were used, and, in most cases, the absorption signal following quadrature Fourier transformation was observed.

Several values of static magnetic field between 1.4 and 8 T were used, and the rotating component of the rf field varied between 30 and 120 G. We will first describe the results of static measurements, line shapes and spectra, and next, those of the spin-lattice relaxation measurements: shape of the recovery curves and temperature dependence.

A. Line shapes and spectra

1. ^{7}Li

The ^{7}Li resonance is quite sharp at high temperatures in all single crystals studied: The observed width is probably mainly due to inhomogeneities in the static magnetic field. Below 100 K, a broadening occurs; below 50 K, a structured seven-line spectrum appears.

For some of several crystals studied, the ^{7}Li NMR linewidth as a function of temperature is shown in Fig. 1. Results on other crystals were similar, if not identical. The evolution of the spectrum as a function of temperature is shown for one crystal in Fig. 2: Note that it can be clearly seen that the quadrupole splitting is independent of temperature, but the spectrum is "averaged out" by in-

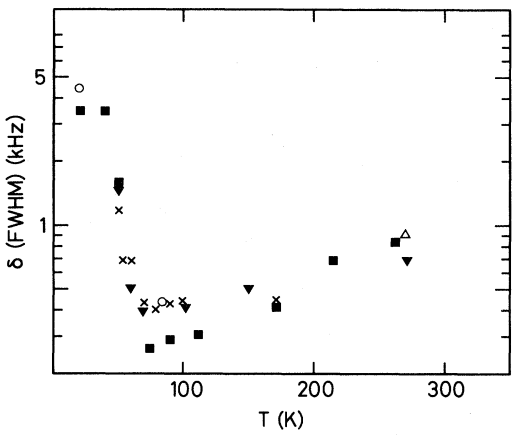

FIG. 1. ^{7}Li NMR linewidth (FWHM) as a function of temperature in $K_{1-x}Li_xTaO_3$: ×, 4.9 at.% (β=90°); Δ, 3.6 at.% (β=45°); ▼, 3.6 at.% (β=90°); ■, 2.6 at.% (β=45°); ○, 2.6 at.% (β=90°). Where a structured spectrum has been observed, the width of the central transition has been plotted. In order to compare the measured width with the theoretical calculations in Eq. (25), one should set $\delta=2\sqrt{2}T_2^{-1}$.

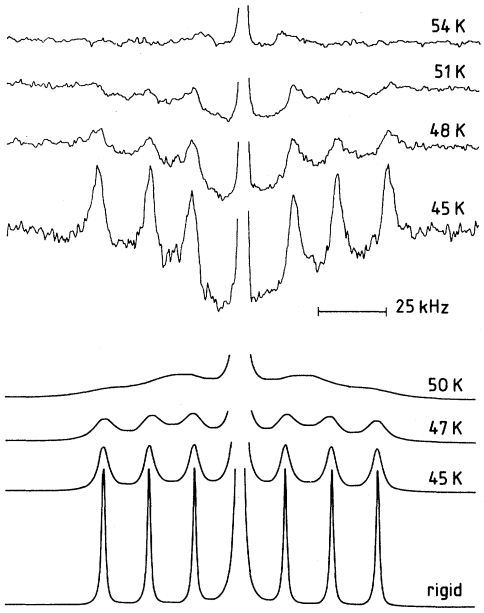

FIG. 2. Evolution of the quadrupole-split NMR spectrum of ^{7}Li in $K_{1-x}Li_xTaO_3$ as a function of temperature for an orientation of $\vec{H}_0$ corresponding to $\alpha=0,\beta=24°$ (see Table I). Top: Experimental results for $x=0.016$. The "hole" in which the lines lie is an experimental artifact. Bottom: Calculated results from a three-site chemical-exchange model using hopping rates derived from T_1 data for $x=0.016$. The bottom spectrum is the assumed "rigid-lattice" spectrum. The agreement between the calculated and observed temperature ranges where the structure disappears, and its approximate independence of x (not shown), indicates that this is due to single-particle dynamics rather than to the polar properties of $KTaO_3$:Li.

creasing the temperature, just as in the well-known cases of disappearance of structure in liquid high-resolution spectra through chemical exchange.

The variation of the spectrum with the orientation of the applied magnetic field with respect to the crystalline axes has been published earlier,[1] and is not repeated here. It shows that the electric-field-gradient (EFG) tensor at the Li site has essentially cylindrical symmetry around the crystalline ⟨100⟩ axes and that three sites exist where the tensors have mutually orthogonal symmetry axes, compatible with the idea that the Li ions are displaced in ⟨100⟩ directions. The magnitudes of the field gradients in the three sites are identical, and are independent of temperature and of Li concentration as well (in the range studied).

2. ^{39}K

The ^{39}K resonance is similarly quite narrow [200 Hz full width at half maximum (FWHM)] at room temperature, and also broadens toward lower temperatures. No structured spectrum has been found down to 35 K (at lower temperatures the spin-lattice relaxation time becomes prohibitively long). At all temperatures, quadrupole echoes can be generated whose widths do not drastically change with temperature even when passing through the transition temperature T_g. From intensity comparisons it seems that the narrow ^{39}K signal corresponds to the central transition $m=+\frac{1}{2}\leftrightarrow m=-\frac{1}{2}$ which is not affected by quadrupolar effects to first order. In the temperature range studied (300–35 K) no second-order shifts have been found at Larmor frequencies of 16 and 5 MHz. The width of the quadrupolar echoes corresponds to a distribution of quadrupole frequencies of a width (FWHM) of at least 6 kHz; the excitation bandwidth may have been insufficient to observe the full distribution.

3. ^{181}Ta

Finally, the ^{181}Ta resonance is quite broader then the other ones at room temperature, approximately 7 kHz. Its behavior as function of temperature is very remarkable: Upon decreasing the temperature the line intensity drops, without observable broadening, to the extent that it is impossible to detect the resonance below $\sim$100 K. Several crystals with different Li content x showed similar behavior: Specifically, the "vanishing" temperature seems to be independent of x (for x sufficiently large; in a pure $KTaO_3$ crystal the Ta-resonance intensity follows Boltzmann's law at least down to 10 K). These results are plotted in Fig. 3. The intensity again corresponds mainly (if not only) to the central transition, as shown by the relative intensities of the quadrupolar echoes, both in the pure and in the doped crystals.

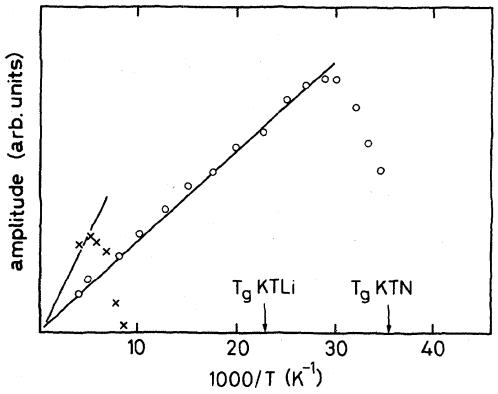

FIG. 3. Intensity of the ^{181}Ta resonance in $K_{1-x}Li_xTaO_3$ (KTLi) and $KTa_{1-x}Nb_xO_3$ (KTN) as a function of inverse temperature. Vertical scale is the amplitude in arbitrary units, not identical for results marked by circles and crosses. Crosses: KTLi ($x=2.4$ at. %). Circles: KTN ($x=1.8$ at. %). The straight line reflects Boltzmann's law.

B. Spin-lattice relaxation

1. ^{7}Li

The spin-lattice relaxation rate T_1^{-1} has been measured by 90°-τ-90° and 180°-τ-90° pulsed sequences. In the temperature range between 90 and 150 K, the ^{7}Li spin-lattice relaxation curve depends on the orientation of the crystal in the static magnetic field, but not on the field's magnitude; such a dependence is observed below $\sim$90 K. For some orientations the relaxation is clearly nonexponential, whereas for other orientations the curves are exponential at all temperatures over the decay range (typically somewhat less then a decade) observed (see Fig. 4). In those cases, T_1^{-1} can be uniquely defined, and, as we have shown before,[1,6] its temperature and frequency dependence can be well described by a Bloembergen-Purcell-Pound–type (BPP-type) formula (Fig. 5). We will derive an expression for the orientation dependence in Sec. III,

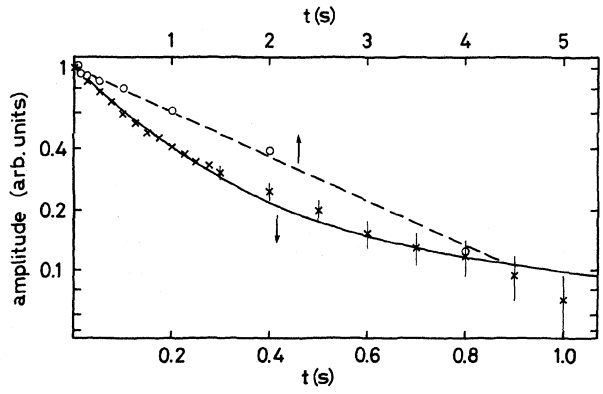

FIG. 4. Relaxation of ^{7}Li in $K_{1-x}Li_xTaO_3$ ($x=0.036$) at two temperatures: logarithm of the signal amplitude after a two-pulse sequence vs pulse spacing t. The lines are described by Eq. (4). Orientation of $\vec{H}_0$ such that $\beta=0$ in Eq. (11), and $W_1=0$ (that is, if the orientation were perfect; the possible error is several degrees). Circles and top scale: $T=174$ K. Here, spin-spin interactions are important ($V/W_2 \gg 1$) and a single decay results. Crosses and bottom scale: $T=125$ K. The spin-lattice couplings are more efficient, and a double decay is observed. The line can be described by $V=W_2/4$, but the exact orientation is important in determining this value.

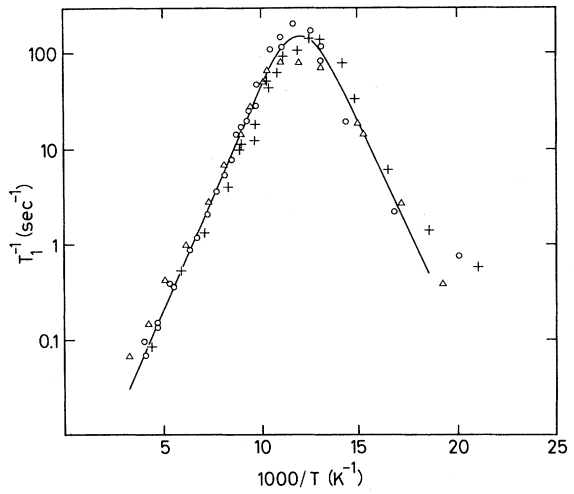

FIG. 5. Spin-lattice relaxation rate of ^{7}Li in KTL as a function of inverse temperature. Pluses, $x=1.1$ at. %; circles, $x=1.6$ at. %; triangles, $x=6.3$ at. %. The theoretical curve represents the best fit according to Eqs. (26) and (27) in the main text.

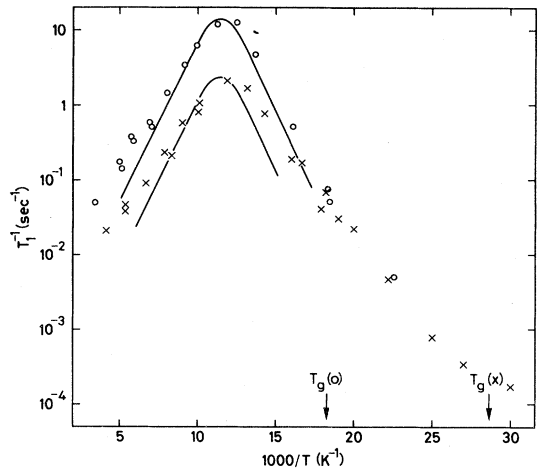

FIG. 7. Spin-lattice relaxation rate of ^{39}K in KTL as a function of inverse temperature. The T_1^{-1} plotted have been obtained from a fit to the long-time tail of the relaxation curve. Circles: $x=4.9$ at. %; crosses: $x=1.6$ at. %. The resonance frequency is $\nu_L=15.3$ MHz. The solid lines are theoretical curves of best fit as explained in the text.

which qualitatively describes the results in Fig. 4. A quantitative fit is, to some extent, arbitrary, since our measurement of the orientation of the field with respect to the crystalline axes is rather crude, probably $\pm 3°$ (compare the rotation diagram in Fig. 3 of Ref. 1).

Measurements of spin-lattice relaxation rate in the rotating frame, $T_{1\rho}^{-1}$, have been performed in one $KTaO_3$:Li crystal as a function of temperature, and are shown in Fig. 6. The unexpected feature of these results is the maximum observed in $T_{1\rho}^{-1}$ at $T>100$ K. It cannot be explained in terms of the same relaxation mechanism which produces the maximum in T_1^{-1}, but rather it indicates the presence of a two—time-scale relaxation mechanism as will be discussed in Secs. IV and V.

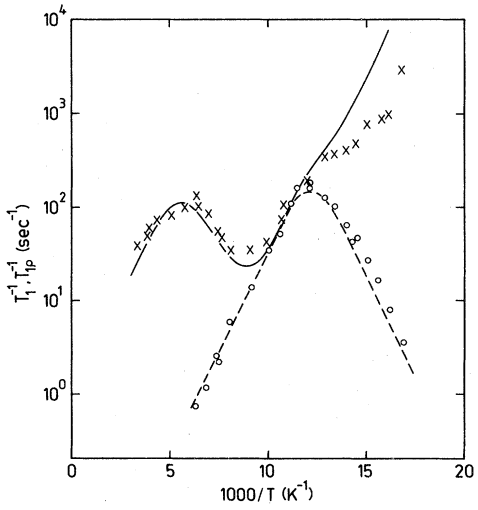

FIG. 6. Spin-lattice relaxation rate in the laboratory and in the rotating frame of ^{7}Li in a KTL sample with $x=1.6$ at. % vs (1000 K)/T. The resonance frequency is $\nu_L=20$ MHz. The rf field is $\omega_1=10^5$ Hz rad ○, T_1^{-1}; ×, $T_{1\rho}^{-1}$. The dashed line is the best fit according to Eqs. (26) and (27), and the solid line is the best fit according to Eqs. (28) and (29).

2. ^{39}K

The ^{39}K spin-lattice relaxation decay curve is nonexponential at temperature above 50 K and independent of orientation. To characterize the curves we have chosen an exponential fit to the long-time tail of the curve (again we observe somewhat less than a decade of decay) and report the time constant so obtained as T_1^{-1} in Fig. 7. Again we see an approximate Arrhenius behavior and fairly short values of the relaxation time, in marked contrast to the T^2 temperature dependence found in pure $KTaO_3$.

III. ^{7}LI RELAXATION PARAMETERS AND LI$^+$ THERMAL MOTION

The hopping of the Li ions between different sites causes both spin-lattice relaxation and the collapse of the quadrupolar-split spectrum. In this section we briefly describe the relationship between the observed NMR parameters (T_1^{-1} and $T_{1\rho}^{-1}$) and parameters describing the dynamics of the Li$^+$ ions (average residence time τ, energy barrier E, rms quadrupole interaction).

In ionic solids, the relaxation transition rates induced by quadrupolar interaction are most frequently due to coupling of lattice vibrations with the nuclear quadrupole moment, at least at lower temperatures, where diffusion is not important. Generally speaking, the anharmonic Raman process is the most effective in causing relaxation, giving a characteristic $T_1^{-1}\propto T^2$ temperature dependence.[7]

Such behavior has been observed,[8] e.g., on the ^{39}K resonance in pure and Na-doped $KTaO_3$, and is very different from the temperature variation shown in Figs. 5 and 7. In systems undergoing classical phase transitions, the direct process, i.e., absorption or emission of a phonon by the spin system, is thought to be the dominant process near the transition temperature, where low-frequency, long-wavelength fluctuations in the order parameter occur.[5] Specifically, at ferroelectric transitions, both of order-disorder and of displacive character, a very marked maximum of the relaxation rate occurs. In such systems, the temperature variation of the order parameter is reflected in the temperature variation of the static quadrupolar splitting of a suitably chosen nuclear resonance, again in contrast to what is experimentally observed for Li in $KTaO_3$ (see Fig. 2) where the rms quadrupole interaction at high temperatures (as derived from the relaxation rates) and the static quadrupole coupling (derived from the spectral splitting at low temperatures) agree well and are, within experimental error, independent of temperature.[1]

From these observations we deduce that the effect of collective fluctuations on the spin-lattice relaxation of Li is largely dominated by the local effects created simply by the displacement of the Li nucleus under observation with respect to the cubic site: the thermally activated hopping between sites is the modulation mechanism. Correlation among Li displacements in different cells gives rise to a smaller quadrupole interaction which is modulated on a longer time scale and can be detected only in the measurements of relaxation rate in the rotating frame, $T_{1\rho}^{-1}$, at relatively high temperature. Deferring a detailed consideration of the hopping dynamics to Sec. IV, in this section we will give a description of the nonexponential recovery observed in presence of spin-lattice and spin-spin relaxation processes of the same order of magnitude and of the relation between the nuclear relaxation transition probabilities W_0, W_1, and W_2, and the correlation function for the fluctuating EFG tensor components.

A. Master equation for spin-lattice relaxation

In the master-equation approach it is assumed that thermal equilibrium between the populations of the four energy levels ($m=\pm\frac{3}{2}$ and $\pm\frac{1}{2}$) of a spin $I=\frac{3}{2}$ in an external field is attained through detailed balance, and it is supposed that the transition rates W_1 (for $\Delta m=\pm1$ transitions) and W_2 ($\Delta m=\pm2$) are proportional to the matrix elements of the quadrupolar interaction between the levels involved. We will introduce an additional transition probability, denoted V, chosen such that it tends to equilibrate the populations without changing the total magnetization. V can be interpreted as a measure for the strength of the spin-spin interactions or for the rate at which a spin temperature is set up.

If it is assumed that the initial state of the spin system is describable by a single spin temperature, as will be the case after complete saturation or population inversion (but not, e.g., after selective saturation), the rate of change of the four populations can be described by two equations,[9]

$$\begin{aligned}\frac{d}{dt}N_{3/2}&=-(W_1+W_2)N_{3/2}+(W_1-W_2)N_{1/2}\ ,\\ \frac{d}{dt}N_{1/2}&=(W_1-W_2)N_{3/2}-(W_1+W_2)N_{1/2}\ ,\end{aligned}\tag{1}$$

where

$$N_m(t)=[n_m(t)-n_m^0]-[n_{-m}(t)-n_{-m}^0]\ ,\tag{2}$$

and $n_m(t)$ is the population at time t of the level with magnetic quantum number m, and n_m^0 is the equilibrium value. Now we introduce additional equations,

$$\begin{aligned}\frac{d}{dt}N_{3/2}&=-\tfrac{1}{10}V(N_{3/2}-3N_{1/2})\ ,\\ \frac{d}{dt}N_{1/2}&=-\tfrac{3}{10}V(-N_{3/2}+3N_{1/2})\ ,\end{aligned}\tag{3}$$

which mean that for $V\to\infty$ we will have $3N_{1/2}=N_{3/2}$ at all times (amounting to the existence of a spin temperature) under the constraint that the time derivative of $3N_{3/2}+N_{1/2}$ vanishes (so that V does not change the total magnetization).

From the solution of these equations we obtain, for the normalized relaxation function $M(t)\sim3N_{3/2}(t)+N_{1/2}(t)$,

$$M(t)=(\tfrac{1}{2}-D)\exp(-\rho_1 t)+(\tfrac{1}{2}+D)\exp(-\rho_2 t)\ ,\tag{4}$$

with

$$\begin{aligned}\rho_1&=W_1+W_2+\tfrac{1}{2}(V+R)\ ,\\ \rho_2&=W_1+W_2+\tfrac{1}{2}(V-R)\ ,\\ D&=[5V+6(W_1-W_2)]/10R\ ,\end{aligned}\tag{5}$$

and R is determined from

$$25R^2=[5V+6(W_1-W_2)]^2+[8(W_1-W_2)]^2\ .\tag{6}$$

Now the spin-temperature result is obtained by letting $V\to\infty$ so that $D=\frac{1}{2}$, $\rho_1\to\infty$, and $\rho_2=(2W_1/5+8W_2/5)$, whereas the limit of no spin-spin interaction ($V=0$) leads to $D=\frac{3}{10}$, $\rho_1=2W_1$, and $\rho_2=2W_2$, in agreement with the result obtained by density-matrix methods.

The general case of $V\neq0$ treated here corresponds, in the density-matrix formalism, to the conditions of thermal mixing among Zeeman levels which occurs in a time of the order of the spin-lattice relaxation time itself. One should then attribute a spin temperature to each pair of Zeeman levels, a situation which is not easy to work out explicitly with the density-matrix formalism.[10]

B. Transition rates

The standard theory of nuclear magnetic relaxation through motion in the weak-collision limit can be easily adapted to the present problems to give[9]

$$W_m=4\pi^2\nu_Q^2\tfrac{1}{2}\int_{-\infty}^{+\infty}g_m(t)\exp(im\omega_0 t)dt\ ,\tag{7}$$

with the correlation function given by

$$g_m(t)=\sum_{i,j}F_{m,i}F_{-m,j}p_i(P_{ij}(t)-p_j)\ ,\tag{8}$$

TABLE I. Irreducible components of the EFG tensor F_m:

$$F_0=V'_{zz}\ ,\quad F_{\pm1}=V'_{xz}\pm iV'_{yz}\ ,\quad F_{\pm2}=\tfrac{1}{2}(V'_{xx}-V'_{yy})\pm V_{xy}\ ,$$

in units of $\frac{1}{2}eq$ and computed for the Li^+ ion displaced along crystal axes x, y, and z, respectively. α and β are the azimuthal and polar angles of the magnetic field $\vec{H}_0$ in the crystal-axis system. The measurements presented in this paper were performed with $\vec{H}_0$ in the x-z plane, i.e., $\alpha=0$.

$$F_0(x)=-\tfrac{1}{2}+\tfrac{3}{2}\sin^2\alpha\sin^2\beta$$
$$F_0(y)=-\tfrac{1}{2}+\tfrac{3}{2}\cos^2\alpha\sin^2\beta$$
$$F_0(z)=-\tfrac{1}{2}+\tfrac{3}{2}\cos^2\beta$$

$$(\tfrac{8}{3})^{1/2}F_1(x)=-\sin2\beta\sin^2\alpha-i\sin\beta\sin2\alpha$$
$$(\tfrac{8}{3})^{1/2}F_1(y)=-\sin2\beta\cos^2\alpha+i\sin\beta\sin2\alpha$$
$$(\tfrac{8}{3})^{1/2}F_1(z)=\sin2\beta$$

$$(\tfrac{8}{3})^{1/2}F_2(x)=-1+\sin^2\alpha(1+\cos^2\beta)+i\sin2\alpha\cos\beta$$
$$(\tfrac{8}{3})^{1/2}F_2(y)=\cos^2\beta-\sin^2\alpha(1+\cos^2\beta)-i\sin2\alpha\cos\beta$$
$$(\tfrac{8}{3})^{1/2}F_2(z)=\sin^2\beta$$

$$F_{-m}=(-1)^mF_m^*$$

where the indices i,j run over the six sites, $m=0,1,2$; the $F_{m,i}$ are given in Table I. The quadrupole coupling frequency is given ($I=\frac{3}{2}$) by

$$\nu_Q=\tfrac{1}{2}[eqQ(1-\gamma_\infty)/h]\ , \tag{9}$$

where q is the largest component of the EFG tensor in the principal-axis frame of reference. If the average $\sum_k p_k F_{m,k}$ is not zero, it should be included in the main Hamiltonian, where those terms with $m=\pm1,\pm2$ do not affect the spectrum in first order.

A model-based calculation of $g(t)$ will be presented in the next section. Here, we express the relaxation transition probabilities in terms of the spectral densities of the reduced correlation function,

$$j_m(\omega)=\tfrac{1}{2}\int_{-\infty}^{+\infty}\frac{g_m(t)}{g_m(0)}\exp(i\omega t)dt\ . \tag{10}$$

In Eq. (8), p_i is the *a priori* probability that the displacement is towards site i, and $P_{ij}(t)$ is the transition probability of finding the ion in site j at time t, given it was in site i at time 0. In order to show the explicit angular dependence of the relaxation transition probabilities we consider the case of isotropic hopping motion of Li ions for which all $p_i=\frac{1}{6}$, and one obtains, from Eqs. (7), (8), and (10),

$$W_1=4\pi^2\nu_Q^2\sin^2\beta\cos^2(\beta)j_1(\omega_0)\ ,$$
$$W_2=4\pi^2\nu_Q^2\tfrac{1}{4}(1-\cos^2\beta\sin^2\beta)j_2(2\omega_0)\ , \tag{11}$$

where β is the polar angle of $\vec{H}_0$ in the cubic crystal-axis system, and the azimuthal angle has been taken as 0.

The complex angular and temperature dependence of the recovery of the nuclear magnetization can be explained by considering the results of Eqs. (4)—(6) with $W_{1,2}$ given in Eq. (11). Above the maximum of T_1^{-1} on the high-temperature side (see Fig. 5), $j(\omega_0)\sim j(2\omega_0)$, and for $\beta=31.7°$ one has $W_1\equiv W_2$, yielding an exponential decay independent of spin-temperature considerations. In the limit of a common spin temperature [$V\to\infty$ in Eqs. (4)—(6)] the recovery is exponential for all angles β. This is the situation found experimentally at room temperature. As the temperature is lowered towards the T_1^{-1} maximum, T_1 decreases, becoming of the order of T_2 (see Figs. 1 and 5). Now we have, in Eqs. (4)—(6), a finite V which may vary as a function of temperature following the change of T_1/T_2. In Fig. 4 the transition from single- to double-exponential relaxation upon lowering the temperature at $\beta=0$ is shown. Here $W_1=0$ (if no other relaxation mechanism exists), and some small, but nonzero V can describe the lower curve. Below the T_1^{-1} maximum on the low-temperature side, $j(\omega_0)\neq j(2\omega_0)$, and, consequently, $W_1\neq W_2$ even for $\beta=31.7°$, yielding a slight nonexponential decay. In this case, the experimental recovery plot is fitted to the longer-time constant W_2^{-1}, which contributes with the larger weight to the recovery of the magnetization in the case of no common spin temperature [see Eq. (4)]. We conclude that in order to analyze the experimental measurements performed here for $\beta=31.7°$, we can assume $T_1^{-1}\simeq 2W_2$ over the entire temperature range.

The recovery of the nuclear magnetization in presence of a rf field H_1 at resonance and stronger then the local dipolar field H_L, $H_1\gg H_L$, yields the spin-lattice relaxation rate in the rotating frame.[10] Since the nuclear spins are now preferentially oriented along the rf field, the relaxation of the magnetization transverse with respect to $\vec{H}_0$ requires the exchange of quanta of energy of the order of $\omega_1=\gamma H_1$. The lattice components F_0 (Table I) are involved because these are connected with the nuclear-spin operator I_z perpendicular to the field $\vec{H}_1$. For isotropic hopping one has

$$W_0=4\pi^2\nu_Q^2\tfrac{1}{2}(1-3\cos^2\beta\sin^2\beta)j(2\omega_1)\ . \tag{12}$$

If a common spin temperature is maintained during the relaxation process a simple exponential decay is obtained with

$$1/T_{1\rho}=\tfrac{1}{5}(\tfrac{9}{2}W_0+5W_1+2W_2)\ . \tag{13a}$$

In the opposite case of negligible thermal mixing among Zeeman levels, the recovery of the nuclear magnetization is obtained by transforming the W_m into the rotating frame to yield

$$M(t)=\tfrac{1}{5}\exp[-(W_1+W_2)t]+\tfrac{4}{5}\exp[-(\tfrac{9}{8}W_0+W_1+W_2/4)t]\ . \tag{13b}$$

For $\beta=31.7°$ and $j(2\omega_1)\sim j(\omega_0)\sim j(2\omega_0)$, the relaxation transition probabilities are all equal and one obtains a nearly exponential recovery with $T_{1\rho}^{-1}\simeq T_1^{-1}$. In the temperature region in which $j(2\omega_1)\gg j(\omega_0)$, the recovery of the nuclear magnetization is entirely dominated by W_0, yielding $T_{1\rho}^{-1}\simeq W_0$ in both Eqs. (13a) and (13b).

IV. DYNAMICS OF Li IONS TWO–TIME-SCALE MOTION

The simplest model one might conceive that shows a temperature dependence with two unrelated maxima for relaxation in the laboratory (T_1^{-1}) and in the rotating ($T_{1\rho}^{-1}$) frames, respectively, is a two–time-scale model. Since the rotating-frame experiments are typically performed in effective magnetic fields of a few gauss, whereas the laboratory-frame experiments are done in fields that may attain tens of kilogauss, the time scales to which the experiments are most sensitive differ by 3 or 4 orders of magnitude. Fast hopping of the Li ions between all sites gives T_1 relaxation and destroys the spectrum, but on this fast time scale, the residence times in the different sites are not equal, corresponding to a type of local ordering or possibly cluster formation.

The equalization of residence times occurs on a longer time scale, and in a certain temperature range this process may dominate the $T_{1\rho}$ relaxation. Whether net effects on the quadrupolar splitting of the spectrum should occur depends on the degree of local ordering and on the magnitude of the slow time scale. From the experimental values for T_1, $T_{1\rho}$, and ν_Q, it follows that in the temperature region of interest, the degree of local ordering is less then 5% and no measurable effects on the spectrum are expected.

To introduce the notation, let us first consider the case of one time scale only. The Li ions are equally distributed over the six possible orientations and may jump from one orientation to any of the four that are at right angles to it, but not to the orientation opposite to it. We label the six potential wells by

$$i=-3,-2,-1,1,2,3$$

such that the ion may in a single jump go from well number i to four other wells, but not to well number $-i$. We describe the hopping from the ith to the jth well as a Poisson process of rate λ_{ij}, and the sequence of indices of successively occupied wells as a Markovian chain of six possible values. To calculate the correlation functions and spectral densities [see Eqs. (8) and (10)] we need the time-averaged probabilities p_i to find the particle in well number i, and the transition probability functions $P_{ij}(t)$, describing the probability that a particle that is initially in the ith well, will be in the jth well at time t. Details of such calculations are given in the Appendix.

If all six orientations are equally probable, of course all $p_i=\frac{1}{6}$, and the transition probability functions are

$$\begin{aligned}P_{ij}(t)=&\tfrac{1}{6}[1-\exp(-3t/2\tau)]\\&+\tfrac{1}{2}(\delta_{ij}+\delta_{-ij})\exp(-3t/2\tau)\\&+\tfrac{1}{2}(\delta_{ij}-\delta_{-ij})\exp(-t/\tau)\ .\end{aligned}\tag{14}$$

The functions $P_{ij}(t)$ govern both dielectric and NMR relaxation processes, but the dielectric relaxation measures the correlation function of a tensor of rank 1 (the direction of the electric-dipole-moment vector), whereas NMR quadrupolar relaxation depends on a second-rank tensor (the EFG tensor). Since the former transforms under the rotations described by $P_{ij}(t)$ as the first-order spherical harmonic, and the latter transforms as a second-order one, the correlation times measured by dielectric and NMR measurements are generally not identical. For the $P_{ij}(t)$ given in Eq. (14) the dielectric relaxation picks out the $\exp(-t/\tau)$ decay since the dipole-moment vector changes sign when the Li ion goes from site i to site $-i$. The EFG tensors in these two sites are identical, however, and the NMR relaxation is sensitive to the $\exp(-3t/2\tau)$ decay only. The correlation times determined by both methods for this $P_{ij}(t)$ therefore differ by a factor of $\frac{3}{2}$. (In Ref. 1 we assumed a factor of 3, as is correct for isotropic diffusional motion, but not for this discrete site hopping model.)

The correlation function for the components F of the EFG tensor as the ion hops between the different sites is given by

$$\begin{aligned}g(t)&=\sum_{i,j}F_iF_j^*p_i(P_{ij}(t)-p_j)\\&=\tfrac{1}{6}\sum_i F_i^2\exp(-3t/2\tau)\ ,\end{aligned}\tag{15}$$

with the $F_i^{(m)}$ given in Table I.

Next, consider a two–time-scale process. To simplify the mathematics, we concentrate on NMR relaxation, where no distinction exists between well number i and well number $-i$. It is therefore sufficient to consider only three "effective" sites, labeled by capital indices. The p_I are not taken to be all equal to $\frac{1}{3}$, and the corresponding P_{IJ} are derived in the Appendix. Focusing on the case of a small degree of local ordering (i.e., small deviations of the p_I from $\frac{1}{3}$) an approximate expression for $P_{IJ}(t)$ is

$$P_{IJ}(t)\approx(\delta_{IJ}-p_J)\exp(-\lambda_1 t)\ ,\tag{16}$$

where λ_1 is approximately given by

$$\lambda_1^{-1}\approx\tfrac{2}{3}\tau_{\rm av}=\tau_c\ ,\tag{17}$$

and $\tau_{\rm av}$ is the average residence time in the six off-center positions.

With this expression for $P_{IJ}(t)$ the fast part $g'(t)$ of the correlation function of the components F of the EFG can be written as

$$\begin{aligned}g'(t)&=\sum_{I,J}F_IF_J^*p_I(P_{IJ}(t)-p_J)\\&=\left[\sum_I p_IF_I^2-\left[\sum_I p_IF_I\right]^2\right]\exp(-\lambda_1 t)\ .\end{aligned}\tag{18}$$

With

$$p_I-\tfrac{1}{3}=d_I\ ,$$

the factor in large square brackets becomes (since $\sum_I F_I=0$)

$$\begin{aligned}&\sum_I p_IF_I^2-\left[\sum_I p_IF_I\right]^2\\&\qquad=\tfrac{1}{3}\sum_I F_I^2+\sum_I d_IF_I^2-\sum_{I,J}d_Id_JF_IF_J^*\ .\end{aligned}\tag{19}$$

Locally, the preferential ordering on the short-time scale is specified by giving the value of d along two axes. We assume the degree of ordering, i.e., the *values* of the pa-

TABLE II. Transition temperature T_g from Ref. 1 for different samples of $K_{2-x}Li_xTaO_3$. T_Q is the temperature at which a quadrupole-split spectrum appears.

Sample[a]	X (at. %)	T_g (K)	T_Q (K)
KSK 11	1.1		40
KSK 18	1.6	34	50
KSK 20	2.4	43	50
KSK 14	2.6	48	
KSK 25	3.6	58	50
KSK 53	4.9	73	
KSK 27	6.3	85	55

[a]The code KSK refers to the growth run [see J. J. van der Klink and D. Rytz, J. Cryst. Growth **56**, 673 (1982)].

rameters d, to be constant in time, but the *direction* of the ordering, i.e., the axes along which the values of d are applicable, to decay on the longer-time scale. At any given moment, we can take an average of Eq. (19) over all of the crystal to describe the effect of the long-time decay, and in doing so the second term on the right-hand side vanishes. The average $\langle d_I d_J \rangle_{\rm av}$ occurring in the third term is

$$\langle d_I d_J \rangle_{\rm av} = \tfrac{1}{6} d^2 (2\delta_{IJ} - 1) , \tag{20}$$

with

$$d^2 = d_x^2 + d_y^2 + d_z^2 .$$

Therefore,

$$\langle g'(t) \rangle_{\rm av} = \tfrac{1}{3}(1-d^2) \sum_I F_I^2 \exp(-\lambda_1 t) . \tag{21}$$

If we finally make the assumption that the decay of the preferential ordering can be described by a simple exponential of a rate λ_3, we have, for the full correlation function $g(t)$,

$$\langle g(t) \rangle_{\rm av} = \langle g'(t) \rangle_{\rm av} + \tfrac{1}{3} d^2 \sum_I F_I^2 \exp(-\lambda_3 t) . \tag{22}$$

The explicit expressions for T_1^{-1} and $T_{1\rho}^{-1}$ are easily obtained by using correlation function (22) in calculating the spectral densities in Sec. III.

It should be noted that the angular dependence of the W_m in Eqs. (11) and (12) is not affected by the anisotropy of the Li dynamics. In this model, for T_1^{-1} one expects two maxima when $\lambda_1^{-1}\omega_0 \sim 1$ and when $\lambda_3^{-1}\omega_0 \sim 1$, respectively. In addition, two maxima are expected for $T_{1\rho}^{-1}$ at $\lambda_1^{-1}\omega_1 \sim 1$ and $\lambda_3^{-1}\omega_1 \sim 1$. The temperature range in which the experiments were performed allow one to observe only the maximum of T_1^{-1} at $\lambda_1^{-1}\omega_0 \sim 1$ and the one of $T_{1\rho}^{-1}$ at $\lambda_3^{-1}\omega_1 \sim 1$, the first being dominated by the fast motion and the second by the slowly relaxing local order. The ratio of the mean-square interactions as determined from the $T_{1\rho}^{-1}$ and T_1^{-1} maxima is a measure for the degree of ordering,

$$\langle \nu_Q^2 \rangle_{T_{1\rho}} / \langle \nu_Q^2 \rangle_{T_1} \approx d^2 .$$

V. INTERPRETATION OF THE RESULTS

The NMR results are discussed in this section in relation to the problem of the nature of the ordering of the electric dipoles formed by the off-center Li ions. The temperature T_g at which dielectric and optical measurements indicate the occurrence of some kind of phase transition are summarized in Table II for the samples investigated in the present work. Also, for sake of convenience, in Table III we summarize the nuclear and ionic properties utilized in the different calculations performed in this section.

A. Static properties

1. ^{7}Li

As mentioned in an earlier paper,[1] the slowing down of the Li motion upon lowering the temperature leads to the appearance of a quadrupole-split spectrum at a temperature that can be related to the experimental spin-lattice relaxation curve through the Kubo-Tomita theory for motional narrowing. A more quantitative description of how the spectrum merges over a narrow temperature interval can be obtained by using chemical-exchange models. As a given ion jumps between different sites, the central transition of the NMR spectrum is not affected to first order. The satellite transitions each occur at one of three distinct frequencies whose average coincides with the central transition, and the chemical-exchange theory can be applied to each transition separately. The problem is similar to that of a reorienting octahedron,[11] and a result of numerical calculations for isotropic Li motion, using the hopping rates given in Ref. 1 for $x = 1.6$ at. %, is shown in Fig. 2.

At low temperature the position of the quadrupole satellites as a function of the orientation of the magnetic

TABLE III. Summary of nuclear properties.

Nucleus	I	Q (10^{-24} cm^2)	$1-\gamma_\infty$	γ_N	Natural abundance (at. %)
^{7}Li	$\frac{3}{2}$	0.042	0.74	1655	92.6
^{39}K	$\frac{3}{2}$	0.055	18	198.7	93
^{181}Ta	$\frac{7}{2}$	65	~100	460	100
^{17}O	$\frac{5}{2}$			577	0.037
^{6}Li	1			626.5	7.4

field $\vec{H}_0$ in the (100) plane is described, for $I=\frac{3}{2}$ and an axially symmetric EFG by[9]

$$\nu_{\pm}=\nu_L\pm(\nu_Q/2)[3\cos^2(\theta)-1]\ , \tag{23}$$

where $\nu_Q=\frac{1}{2}(e^2qQ/h)$ and the maximum component eq of the EFG forms the angle θ with $\vec{H}_0$. The magnitude of the quadrupole frequency ν_Q can be related to the amount of off-center displacement δ of the Li ion by computing the EFG in a point-charge approximation. The estimate of the EFG based on expansions in terms of δ/a is slowly converging for $\delta/a>0.1$, leading to erroneous results if limited to the quadratic term.[1] A numerical calculation based on a lattice summation over $41\times41\times41$ cells around a given Li nucleus indicates[12] that the EFG reaches a minimum for $\delta\simeq0.65$ Å and reverses sign for $\delta\simeq0.8$ Å. The experimental value of $\nu_Q=70$ kHz corresponds to $\delta=1.26$ Å, in good agreement with a theoretical calculation of the off-center Li equilibrium position in a polarizable point-charge model for the $KTaO_3$ lattice.[12]

Next, we consider the EFG generated at the ^{7}Li site by the random distribution of "frozen" Li off-center ions in neighboring cells. This "intercell" contribution could produce an inhomogeneous quadrupole broadening of the satellite lines and of the central line in the quadrupole-split spectrum. However, in the present case, the second-order effect is negligible, while the first-order effect on the satellite lines is only a few kilohertz for the first few neighbors which have negligible statistical weight in samples with $x<0.1$.

Finally, we can observe that in the highest-concentration samples (see Table II) the transition temperature T_g falls well above the temperature at which the quadrupole-split spectrum appears, namely 40–55 K. Thus the transition cannot be ascribed to a sudden "freezing" of the off-center Li ions. It remains to be established if the transition can be associated to a tetragonal distortion of the lattice similar to the one occurring in other perovskite systems such as, e.g., $KNbO_3$ or $SrTiO_3$. The ν_Q can be related to the c/a ratio by using a point-charge approximation. The result is slightly different for a distortion due to a rotation of the TaO_3 octahedra, or for a shift of the cubic Ta sublattice against the O sublattice (Slater mode),

$$\nu_Q=385\left[\frac{c-a}{a}\right]\ \text{(rotation of octahedra)}\ ,$$

$$\nu_Q=227\left[\frac{c-a}{a}\right]\ \text{(Slater mode)}\ ,$$

in units of kHz. In order to escape experimental detection the tetragonal distortion should be $(c-a)/a<0.02$, producing a first-order splitting which falls within the ^{7}Li linewidth (see Fig. 1).

The second moment of the ^{7}Li-resonance line is computed with the use of the Van Vleck formula,[9]

$$\langle(\Delta\omega)^2\rangle=\tfrac{3}{4}\gamma^4\hbar^2I(I+1)\sum_k\frac{(1-3\cos^2\theta_k)^2}{r_k^6}\ , \tag{24}$$

for the contribution of like spins, and a similar one with $\frac{3}{4}\gamma^4$ replaced by $\frac{1}{3}\gamma_I^2\gamma_s^2$ is used for the contribution of unlike spins. Here, γ_I is the ^{7}Li gyromagnetic ratio and γ_s is, in turn, the gyromagnetic ratio of ^{39}K, ^{90}Ta, ^{6}Li, and ^{17}O. The second moments have been obtained by summing exactly over nearest neighbors and estimating approximately the contribution of more distant nuclei. For a Gaussian free-precession decay $f(t)\propto\exp(-t^2/T_2^2)$, the transverse relaxation rate T_2^{-1} is related to the second moment of the line by

$$T_2^{-1}=(\sqrt{2}/2)[\langle(\Delta\omega)^2\rangle]^{1/2}\ .$$

The results are

$$\begin{aligned}T_2^{-1}&=0.5+9\sqrt{x}+0.65\sqrt{1-x}\ ,\quad \alpha=0^\circ,\beta=90^\circ\\ T_2^{-1}&=3.5+5\sqrt{x}+0.4\sqrt{1-x}\ ,\quad \alpha=0^\circ,\beta=45^\circ\end{aligned} \tag{25}$$

in units of kHz rad^{-1}, where the concentration-independent contribution comes from Ta nuclei, and x is the relative fraction of Li with respect to K atoms. The angle β denotes the orientation of the magnetic field in the (100) plane with respect to the $\langle100\rangle$ axis. One should notice that the off-center displacement of Li produces only a small modulation of the dipolar interaction and can therefore be neglected. Furthermore, the atomic diffusion is effective in narrowing the line only above room temperature. Above liquid-nitrogen temperature the experimental linewidth is consistently smaller than the theoretical prediction (see Fig. 1).

Around the temperature T_Q at which static quadrupole effects start appearing, the widths of both the central component and the satellite lines are dominated by lifetime broadening due to process of averaging the quadrupole perturbed spectrum. Well below T_Q, the widths of the central line and of the satellite lines are still given by the dipolar interaction. For the central line the theoretical calculation should be multiplied by a correction factor smaller then unity.[13] The same should be true for the satellite width even though no explicit calculation was made in this case.

The experimental value for the linewidth shown in Fig. 1 is in substantial agreement with the rigid-lattice second moment [Eq. (25)] only below liquid-nitrogen temperature. We ascribe the anomalous temperature dependence to a partial averaging out, at higher temperature, of the Ta contribution due to a very fast ^{181}Ta relaxation (T_1 for Ta could very well be of the order of 10^{-5} sec due to the large quadrupole coupling constant).

2. ^{39}K

The ^{39}K NMR spectrum and linewidth described in Sec. II is entirely consistent with a signal perturbed by the quadrupole interaction generated by the randomly situated Li dipoles. The quadrupole coupling constant for the first neighbors is of the order of 10^2 kHz, producing a complete elimination of the satellites and a second-order broadening of the order of a few hundred hertz, in agreement with the broadening observed experimentally at low temperature. On the other hand, the failure to observe any second-order shift of the central line at T_g sets an

upper limit for a possible tetragonal distortion. Under the same approximations as for the ^{7}Li case one finds, for the second-order shift (at $\nu_L = 5$ MHz),

$$\Delta\nu_2 = \frac{3}{16}\frac{\nu_Q^2}{\nu_L} = \begin{cases} 5.6\left[\dfrac{c-a}{a}\right]^2 & \text{(rotation of octahedra)} \\ 1.96\left[\dfrac{c-a}{a}\right]^2 & \text{(Slater mode)}, \end{cases}$$

in units of MHz, which is within the experimental linewidth only for $(c-a)/a < 0.007$.

3. ^{181}Ta

The disappearance of the ^{181}Ta NMR signal shown in Fig. 3 is evidence for the onset of strong inhomogeneous quadrupole interactions. According to the "motional-narrowing" concept, a quadrupole interaction of strength ν_Q becomes static when the correlation time τ_c is of the order of ω_Q^{-1}. The quadrupole interaction at a ^{181}Ta site due to an off-center nearest-neighbor (NN) Li is $\nu_Q \simeq 40$ MHz which should be regarded as an order of magnitude in view of the poor knowledge of the parameters for ^{181}Ta in Table III. The correlation time for the Li hopping motion as derived in next section from T_1^{-1} measurements is given by $\tau_c = 2\times10^{-14}\exp[(1000\text{ K})/T]$. Thus if the disappearance of the signal were to be attributed to the Li dipoles it should start at $T \sim 80$ K where $\tau_c \sim \omega_Q^{-1}$. The discrepancy with the data in Fig. 3 appears to be outside the uncertainty of the above estimate. We will show in the following that the ^{181}Ta data, together with the ^{7}Li $T_{1\rho}^{-1}$ data, are consistent with the idea of a small preferential ordering of the Li dipoles decaying slowly in time.

B. Dynamic properties

1. ^{7}Li

The nuclear-spin-lattice relaxation rates shown in Fig. 5 can be fitted by using the theoretical expressions discussed in Secs. III and IV. From Eqs. (10), (11), and (22) one has, for $\beta = 31.7°$,

$$T_1^{-1} \simeq 2W_2 = \tfrac{2}{5}4\pi^2\nu_Q^2\left[(1-d^2)\frac{\tau_c}{1+4\omega_L^2\tau_c^2} + d^2\frac{\tau_s}{1+4\omega_L^2\tau_s^2}\right], \tag{26}$$

where $\tau_c = \lambda_1^{-1}$ and $\tau_s = \lambda_3^{-1}$.

In this temperature range of the experiments the slow decay of the correlation function associated with the small degree of preferential ordering has negligible effects on T_1^{-1} [second term in large parentheses of Eq. (26)]. One should also note that no detectable anomaly and/or enhancement of T_1^{-1} takes place around the temperature T_g, even for samples for which $T_g > T_Q$. The T_1^{-1} data are consistent with a spin-lattice relaxation entirely dominated by the quasireorientational hopping dynamics of the Li ions among the six off-center positions with a correlation time given by

$$\tau_c = 2\times10^{-14}\exp[(1000\text{ K})/T] \tag{27}$$

and a rms quadrupole interaction $[\nu_Q^2(1-d^2)]^{1/2} = 70$ kHz. The hopping dynamics appears to be almost independent of Li concentration corroborating the conclusion that it is largely dominated by the single-particle properties.

The spin-lattice relaxation rates in the rotating frame $T_{1\rho}^{-1}$ shown in Fig. 6 can also be fitted by using the correlation function in Eq. (22). As discussed in Sec. III the existence of a common spin temperature becomes almost irrelevant for measurements performed at $\beta = 31.7°$, where one can assume $T_{1\rho}^{-1} \simeq \frac{9}{8}W_0 + W_1 + \frac{1}{4}W_2$:

$$T_{1\rho}^{-1} = \tfrac{1}{5}4\pi^2\nu_Q^2\left[(1-d^2)\left[\frac{9}{8}\frac{\tau_c}{1+4\omega_1^2\tau_c^2} + \frac{\tau_c}{1+\omega_L^2\tau_c^2} + \frac{1}{4}\frac{\tau_c}{1+4\omega_L^2\tau_c^2}\right] + d^2\left[\frac{9}{8}\frac{\tau_s}{1+4\omega_1^2\tau_s^2}\right]\right]. \tag{28}$$

For temperatures below ~ 120 K, $T_{1\rho}^{-1}$ is dominated, as is T_1^{-1}, by the fast-decaying part of the correlation function describing the quasi-isotropic Li hopping dynamics, while for $T > 120$ K the slow-decaying part of the correlation function, described by the second term in the large square brackets of Eq. (28), prevails.

From the fit of the data indicated in Fig. 6, one obtains

$$\tau_s = 2\times10^{-8}\exp[(1000\text{ K})/T]\ ,\quad (\nu_Q^2 d^2)^{1/2} = 2.3\text{ kHz}\ . \tag{29}$$

The overall fit appears to be satisfactory with the parameters chosen, even though a sizeable discrepancy remains at low temperature. The discrepancy is probably due mostly to the difficulty in performing reliable $T_{1\rho}$ measurements in this temperature range, where the recovery of the nuclear magnetization is nonexponential.

The large prefactor in the activated correlation time τ_s confirms that the dynamical process considered is not a simple single-particle Debye-type relaxation. It is likely that a fit could also be obtained with a different correlation function, such as one describing a distribution of activation energies. It should also be pointed out that below the $T_{1\rho}^{-1}$ maximum, where Eq. (28) predicts $T_{1\rho} \propto \omega_1^2$, we failed to observe this law with different H_1 fields ranging from 5 to 20 G. By combining the results for the rms quadrupole interaction obtained from T_1^{-1} and $T_{1\rho}^{-1}$ measurements, we obtain a degree of preferential ordering of about 3.3%. The parameter d could be considered a kind of order parameter describing the glasslike characteristics

found in these random dipole systems.[1] In particular, if $\lim_{t\to\infty}\langle d(t)d(0)\rangle\neq 0$, the system should display a permanent electric polarization even though the Li dipoles keep reorienting almost isotropically with single-particle–type dynamics. The static quadrupole effects arising from the anisotropy in the Li reorientational motion are sufficiently small to be undetectable in the NMR spectrum.

2. ^{39}K

Since the satellite transitions are eliminated from the ^{39}K NMR spectrum at all temperatures investigated, the irradiation and detection of the nuclear magnetization refer to the central line only. Under these circumstances the recovery of the nuclear magnetization is given by the normalized relaxation function

$$M(t)=\tfrac{1}{2}\exp(-2W_1t)+\tfrac{1}{2}\exp(-2W_2t)\ , \tag{30}$$

in agreement with the nonexponential decay observed experimentally. Assuming that between 50 and 150 K the relaxation is dominated by the hopping of Li-induced dipoles, one can estimate the relaxation transition probabilities from Eq. (7) and using the fast-decaying part of the $g(t)$ in Eq. (22):

$$W_m\sim 4\pi^2\langle\nu_Q^2\rangle\frac{\tau_c}{1+m\omega_L^2\tau_c^2}\ . \tag{31}$$

Since the relaxation rates shown in Fig. 7 were obtained from the slower component in the recovery of the nuclear magnetization, the data can be fitted by assuming $T_1^{-1}=2W_2$. The theoretical curves in Fig. 7 correspond to Eq. (31) with the following choice of parameters:

$$\begin{aligned}&\tau_c=6\times10^{-14}\exp[(1000\text{ K})/T]\ ,\\ &\langle\nu_Q^2\rangle^{1/2}=8.5\text{ kHz}\quad(x=4.9\text{ at. \%})\ ,\\ &\langle\nu_Q^2\rangle^{1/2}=3.5\text{ kHz}\quad(x=1.6\text{ at. \%})\ .\end{aligned} \tag{32}$$

At the low- and high-temperature ends of Fig. 7 the effect of the Raman process becomes important. Most of the remaining discrepancy between the fitted curve and the experimental points can be ascribed to the experimental and theoretical uncertainties when dealing with nonexponential relaxation. The temperature dependence of τ_c is in good agreement with the one derived from ^{7}Li data. The rms interaction is of the order of the quadrupole interaction generated by nearest- and next-nearest-neighbor Li, scaled by $x^{1/2}$, as one would expect for a fluctuating EFG generated by the uncorrelated motion of Li dipoles. For a crystal with $T_g\approx 34$ K, at which the experimental value of T_1 is about 5×10^3 sec, no critical enhancement of the spin-lattice relaxation was observed.

3. ^{181}Ta

The disappearance of the ^{181}Ta signal at relatively high temperature (see Fig. 3) is consistent with a slowly fluctuating preferential ordering. In fact, assuming that the static interaction at the ^{181}Ta nucleus is also roughly reduced to 3.3% of the full interaction with a Li NN, namely $\nu_Q=1.3$ MHz, and by using the correlation time in Eq. (29), one finds that the motional narrowing condition $\tau_c\sim[15(\nu_Q^2/\nu_L)]^{-1}$ is met at $T\sim 170$ K, in excellent agreement with the experiments (see Fig. 3). It should be pointed out that in this case the correlation time should be compared to the second-order quadrupole shift since only the ^{181}Ta central line is observed, and also since the quadrupole interaction considered here is smaller than the resonance frequency used in the experiment: ($\nu_Q=1.3$ MHz) $<$ ($\nu_L=10$ MHz).

VI. DISCUSSION

We have shown that some of the NMR properties of ^{7}Li, ^{39}K, and ^{181}Ta in $KTaO_3$:Li should be ascribed to NMR effects (existence or nonexistence of a common spin temperature; destruction of spectral structure by thermal motion), but that others bear directly upon the polar properties of these crystals (upper limit for tetragonal distortion, absence of critical slowing down, two–time-scale hopping of Li ions). Here, we will briefly discuss the relation between the latter group of data and other experimental and theoretical results on $K_{1-x}Li_xTaO_3$.

The upper limit for a tetragonal distortion, such as found in $BaTiO_3$, is $(c-a)\leq 0.03$ Å at $x=0.049$ ($T_g=73$ K) and at $T\geq 30$ K. From birefringence data on a zero-field-cooled sample with $x=0.026$, the saturation polarization P_s has been derived[4] as 70 mC/m^2. It has been shown on theoretical grounds that such values cannot be obtained by the mere alignment of the Li dipoles and their associated lattice polarization.[12] Writing $P=6ed/a^3$, where d is the distance between the centers of gravity of positive and negative charges in the unit cell of volume a^3, gives $d\approx 0.045$ Å; at 45 K this value would be approximately halved.[4] Our data for static quadrupole effects can therefore be considered as compatible with the birefringence data cited.

The lack of critical effects in the spin-lattice relaxation is a strong argument against the occurrence of a phase transition, be it a displacive one in the host lattice or an order-disorder one in the impurity dipole system. In both cases a singularity in T_1 is expected theoretically,[14] and has been experimentally observed in perovskites,[15] in many members of the potassium dihydrogen phosphate family[16] and in other ferroelectric systems.[14] It has also been observed in the ^{39}K spin-lattice relaxation in a $KTa_{1-x}Nb_xO_3$ crystal near the quantum-ferroelectric regime, where the values of the transition temperature and saturation polarization are comparable to those found in $KTaO_3$Li.[17] The only other known case where no critical effects are observed[8] is $KTaO_3$:Na, which, in several respects, is thought to be similar to $KTaO_3$:Li. At an order-disorder transition the singularity in T_1^{-1} is expected to be logarithmic for anisotropic interactions between the dipoles,[14] and to follow a power law in isotropic cases.[18] It has recently been stated[19] that (for a dipolar interaction modified by the host lattice) the singularity is "only" logarithmic, and therefore should be difficult to detect experimentally. There is no experimental evidence for this assertion; logarithmic singularities have been observed in many order disorder transitions.[5,20,21] An

order-disorder transition in the Li dipole system should slow down the Li dynamics and be visible as a deviation of the single-particle hopping observed. For the ^{39}K data shown in Fig. 7 for the $x=0.016$ case there is no reason to believe that the singularity is masked by other processes either; so our data are not compatible with the occurrence of critical slowing down at T_g.

The time-scale and temperature variation of the Li hopping rate shows that the process is thermally activated, classical motion over barriers, and the observation of a quadrupole-split spectrum shows that there is no tunneling. This implies that, at least below 100 K, the Li ions cannot follow the polarization of the soft mode in the host lattice, that occurs at much higher frequencies. The proposed indirect dipole-dipole coupling between Li dipoles, mediated by soft phonons,[22] is therefore unlikely to be an important mechanism in $KTaO_3$:Li.

The observed two–time-scale motion for the Li hopping fits well into a description in terms of slowly relaxing clusters that grow with decreasing temperature. At some point these clusters may become coupled to the host lattice polarization over sufficient scales of time and space, so that optical effects appear, without a critical slowing down becoming observable in magnetic resonance experiments.

ACKNOWLEDGMENTS

We gratefully acknowledge the fruitful collaboration with D. Rytz and U. T. Höchli on the properties of $KTaO_3$:Li crystals, and would also like to thank A. Rigamonti and A. Châtelain for many clarifying discussions and comments. The crystals used were grown by D. Rytz at the Swiss Federal Institute of Technology.

APPENDIX

We denote by p_i (where i runs over the values $-3,-2,-1,1,2,3$) the time-averaged probability to find the particle in well number i. For six equal wells, of course $p_i=\frac{1}{6}$ independent of i, but in the more general case,

$$p_i \sim \exp(-E_i/kT) \tag{A1}$$

and

$$\sum_i p_i = 1 , \tag{A2}$$

where E_i is the depth of the ith well. We make the usual assumption that the hopping from the ith to the jth well is a Poisson process of rate λ_{ij} and that the sequence of indices of successively occupied wells forms a Markovian chain of six possible values.

Five general relations between the 30 λ_{ij} and the six p_i are given by the requirement that the latter be stationary,

$$\sum_{k\,(\neq j)} (p_k\lambda_{kj} - p_j\lambda_{jk}) = 0 , \tag{A3}$$

which can be considered a slight generalization of the principle of detailed balance.

Finally, we introduce the transition probability functions $P_{ij}(t)$, describing the probability that a particle that is initially in the ith well, will be in the jth well at time t. For very-short-time intervals Δt, their relation to the λ_{ij} is simply

$$\begin{aligned} P_{ij}(\Delta t) &= \lambda_{ij}\Delta t \quad \text{if } i\neq j , \\ P_{ii}(\Delta t) &= 1 - \sum_j \lambda_{ii}\Delta t = 1 + \lambda_{ij}\Delta t , \end{aligned} \tag{A4}$$

where the last relation defines λ_{ii}. Going to the limit $\Delta t \to 0$ one obtains the Chapman-Kolmogorov equation,

$$\frac{dP_{ij}}{dt} = \sum_k P_{ik}(t)\lambda_{kj} . \tag{A5}$$

For six wells of equal depth, the 36 λ_{ij} are given by

$$\lambda_{ij} = \tfrac{1}{4}\tau^{-1}(1 - 5\delta_{ij} - \delta_{-ij}) , \tag{A6}$$

where τ is the average residence time in each well.

The solution for the P_{ij} is

$$\begin{aligned} P_{ij}(t) = {} & \tfrac{1}{6}[1-\exp(-3t/2\tau)] + \tfrac{1}{2}(\delta_{ij}+\delta_{-ij})\exp(-3t/2\tau) \\ & + \tfrac{1}{2}(\delta_{ij}-\delta_{-ij})\exp(-t/\tau) , \end{aligned} \tag{A7}$$

which is used in Eq. (14) of the main text.

To calculate nuclear magnetic relaxation (but *not* dielectric relaxation) for the case where not all p_i are equal, we use the fact that the EFG's in sites that are related by 180° jumps are identical, and that the elements $\lambda_{i,-i}$ for transitions between such sites are supposed to be zero. The diagonal elements λ_{ij} are related to the average residence time τ_i in orientation i by

$$-\lambda_{ii}^{-1} = \tau_i = p_i \sum_j \tau_j . \tag{A8}$$

From now on, we consider only *three* "effective" sites $I=X,Y,Z$ with their three occupancies p_I given by

$$p_I = p_i + p_{-i} , \tag{A9}$$

and their nine transition rates λ_{IJ} related to the λ_{ij} by

$$\lambda_{IJ} = (p_i/p_I)(\lambda_{ij}+\lambda_{i-j}) + (p_{-i}/p_I)(\lambda_{-ij}+\lambda_{-i-j}) . \tag{A10}$$

Because jumps through 180° do not occur, these p_i and λ_{IJ} are still normalized as in Eq. (A2) and fulfill the stationarity conditions in Eq. (A3). From the latter it follows that

$$\lambda_{IJ} = \frac{1-3\delta_{IJ}}{\tau_i+\tau_{-i}} , \tag{A11}$$

which, for $I\neq J$, does depend on I but not on J. The solution of the Chapman-Kolmogorov equation, Eq. (A5), for the λ_{IJ} given by Eq. (A11), is

$$\begin{aligned} P_{IJ}(t) - p_J = {} & \Delta^{-1}[\lambda_2(\delta_{IJ}-p_J)+\lambda_{IJ}]\exp(-\lambda_1 t) \\ & - \Delta^{-1}[\lambda_1(\delta_{IJ}-p_J)+\lambda_{IJ}]\exp(-\lambda_2 t) , \end{aligned} \tag{A12}$$

where the parameters λ_1, λ_2, and Δ are determined by

$$3(\lambda_1+\lambda_2)=(p_X^{-1}+p_Y^{-1}+p_Z^{-1})\lambda_0 ,$$

$$\lambda_1\lambda_2=\lambda_0^2(27p_Xp_Yp_Z)^{-1} ,$$

$$\lambda_0=9\left[\sum_i \tau_i\right]^{-1}=3\tau_{\rm av}/2 , \tag{A13}$$

$$\Delta=\lambda_2-\lambda_1 ,$$

and p_X, etc. defined by Eq. (A9).

Assuming $\Delta>0$, we can rewrite this equation in less symmetric form,

$$P_{IJ}(t)-p_J=(\delta_{IJ}-p_J)\exp(-\lambda_1 t) + \left[\left[\lambda_1-\frac{\lambda_0}{3p_I}\right]\delta_{IJ}+\left[\frac{\lambda_0}{3p_I}-\lambda_1 p_J\right]\right] \times\frac{1-\exp(-\Delta t)}{\Delta}\exp(-\lambda_1 t) . \tag{A14}$$

The two terms in the large square brackets are on the average of the order Δ. If Δ is much smaller than λ_1, the factor $1-\exp(-\Delta t)$ has a value close to 0 in the time interval where $\exp(-\lambda_1 t)$ is not small. Therefore, for sufficiently small Δ/λ_1, i.e., a sufficiently small degree of local ordering,

$$P_{IJ}(t)-p_J\approx(\delta_{IJ}-p_J)\exp(-\lambda_1 t) , \tag{A15}$$

which has been used in Eq. (16) of the main text.

[1]J. J. van der Klink, D. Rytz, F. Borsa, and U. T. Höchli, Phys. Rev. B **27**, 89 (1983).

[2]L. L. Chase, E. Lee, R. L. Prater, and L. A. Boatner, Phys. Rev. B **26**, 2759 (1982).

[3]Y. Yacoby, A. Agranat, and I. Ohana, Solid State Commun. **45**, 757 (1983).

[4]E. Courtens, J. Phys. C **14**, L37 (1981).

[5]F. Borsa and A. Rigamonti, in *Magnetic Resonance of Phase Transitions,* edited by F. J. Owens, H. A. Farach, and C. P. Poole (Academic, New York, 1979).

[6]F. Borsa, U. T. Höchli, J. J. van der Klink, and D. Rytz, Phys. Rev. Lett. **45**, 1884 (1980).

[7]J. van Kranendonk and M. B. Walker, Can. J. Phys. **46**, 2441 (1968).

[8]J. J. van der Klink and D. Rytz, Phys. Rev. B **27**, 4471 (1983).

[9]A. Abragam, *The Principles of Nuclear Magnetism* (Oxford University Press, Oxford, 1961).

[10]D. Wolf, *Spin Temperature and Nuclear Spin Relaxation in Matter,* (Oxford University Press, Oxford, 1979).

[11]H. W. Spiess, Nucl. Mag. Reson. Basic Principles Prog. **15**, 55 (1978).

[12]J. J. van der Klink and S. N. Khanna, Phys. Rev. B **29**, 2415 (1984).

[13]K. Kambe and J. K. Ollom, J. Phys. Soc. Jpn. **11**, 50 (1956).

[14]G. Bonera, F. Borsa, and A. Rigamonti, Phys. Rev. B **2**, 2784 (1970).

[15]G. Bonera, F. Borsa, and A. Rigamonti, in *Proceedings of the XVIIth Colloque Ampère, Turku, 1972,* edited by V. Hovi (North-Holland, Amsterdam, 1973).

[16]R. Blinc, in *Magnetic Resonance of Phase Transitions,* edited by F. J. Owens, C. P. Poole, and H. A. Farach (Academic, New York, 1979).

[17]J. J. van der Klink, work presented at the 5th European Meeting on Ferroelectricity (Malaga, 1983) (unpublished).

[18]R. Blinc, S. Zumer, and G. Lahajnar, Phys. Rev. B **1**, 4456 (1970).

[19]B. E. Vugmeister and M. D. Glinchuk, Solid State Commun. **48**, 503 (1983).

[20]A. Rigamonti, in *Local Properties at Phase transitions,* edited by K. A. Müller and A. Rigamonti (North-Holland, Amsterdam, 1976).

[21]J. L. Bjorkstam, Adv. Magn. Reson. **7**, 1 (1974).

[22]B. E. Vugmeister and M. D. Glinchuk, Zh. Eksp. Teor. Fiz. **79**, 947 (1980) [Sov. Phys.—JETP **52**, 482 (1980)].